



First observation of the decay

$$\Lambda_b^0 \rightarrow \eta_c(1S)pK^-$$

LHCb collaboration[†]

Abstract

The decay $\Lambda_b^0 \rightarrow \eta_c(1S)pK^-$ is observed for the first time using a data sample of proton-proton collisions, corresponding to an integrated luminosity of 5.5 fb^{-1} , collected with the LHCb experiment at a center-of-mass energy of 13 TeV. The branching fraction of the decay is measured, using the $\Lambda_b^0 \rightarrow J/\psi pK^-$ decay as a normalization mode, to be $\mathcal{B}(\Lambda_b^0 \rightarrow \eta_c(1S)pK^-) = (1.06 \pm 0.16 \pm 0.06_{-0.19}^{+0.22}) \times 10^{-4}$, where the quoted uncertainties are statistical, systematic and due to external inputs, respectively. A study of the $\eta_c(1S)p$ mass spectrum is performed to search for the $P_c(4312)^+$ pentaquark state. No evidence is observed and an upper limit of

$$\frac{\mathcal{B}(\Lambda_b^0 \rightarrow P_c(4312)^+ K^-) \times \mathcal{B}(P_c(4312)^+ \rightarrow \eta_c(1S)p)}{\mathcal{B}(\Lambda_b^0 \rightarrow \eta_c(1S)pK^-)} < 0.24$$

is obtained at the 95% confidence level.

Published in Phys. Rev. D102 (2020) 112012

© 2020 CERN for the benefit of the LHCb collaboration. CC BY 4.0 licence.

[†]Full author list given at the end of the paper.

The existence of baryons comprising four quarks and an antiquark was proposed by Gell-Mann [1] and Zweig [2]. Hereafter, these states are referred to as pentaquarks [3]. Two pentaquark candidates were observed in the $J/\psi p$ system of $\Lambda_b^0 \rightarrow J/\psi p K^-$ decays (charge conjugation is implied throughout the text) in a data sample collected with the LHCb experiment during the 2011-2012 data-taking period [4]. These candidates were labeled $P_c(4450)^+$ and $P_c(4380)^+$. Using a larger data sample of $\Lambda_b^0 \rightarrow J/\psi p K^-$ decays, a new pentaquark state, $P_c(4312)^+$, was observed, and the broad $P_c(4450)^+$ structure resolved into two narrower overlapping structures, labeled $P_c(4440)^+$ and $P_c(4457)^+$ [5]. Many theoretical models have been proposed to describe the dynamics of the observed states, including tightly bound $duuc\bar{c}$ pentaquark states [6–12], baryon-meson molecular states [13–21], or peaking structures due to triangle-diagram processes [22–25]. More experimental and theoretical scrutiny is required to verify these models.

The yet-unobserved $\Lambda_b^0 \rightarrow \eta_c p K^-$ decay, where η_c refers to the $\eta_c(1S)$ meson, can provide a unique approach to search for new pentaquarks, and to study the observed states. It has been predicted that a $\bar{D}\Sigma_c$ molecular state, with a mass of around $4265 \text{ MeV}/c^2$, can contribute to the decay $\Lambda_b^0 \rightarrow \eta_c p K^-$ via $\eta_c p$ final-state interactions [26]. The observed $P_c(4312)^+$ state could be such a molecular state [27], since its mass is close to the $\bar{D}\Sigma_c$ threshold [5].

The study of the $\Lambda_b^0 \rightarrow \eta_c p K^-$ decay provides a new way to test the binding mechanism of pentaquark states, as the predicted ratio of the branching fractions for a pentaquark decaying into $\eta_c p$ compared to the $J/\psi p$ final states depends on the pentaquark model. The branching fraction of $P_c(4312)^+ \rightarrow \eta_c p$ is predicted to be 3 times larger than that of the $J/\psi p$ decay mode if the $P_c(4312)^+$ state is a $\bar{D}\Sigma_c$ molecule [13–15].

This paper presents the first observation of the $\Lambda_b^0 \rightarrow \eta_c p K^-$ decay, with the η_c meson reconstructed using the $\eta_c \rightarrow p\bar{p}$ decay mode, and reports a search for the $P_c(4312)^+$ pentaquark state in the $\eta_c p$ system. The analysis uses the decay $\Lambda_b^0 \rightarrow J/\psi p K^-$ as a normalization channel, where the J/ψ meson decays to $p\bar{p}$. The data sample used in this analysis corresponds to an integrated luminosity of 5.5 fb^{-1} , collected with the LHCb experiment in proton-proton collisions at $\sqrt{s} = 13 \text{ TeV}$ between 2016 and 2018.

In the B -meson sector, heavy quark effective theory [28, 29] predicts that the decay rates of the $B \rightarrow \eta_c X$ and $B \rightarrow J/\psi X$ channels are of the same order of magnitude. Experimental results are in good agreement with this expectation [30]. Studying the branching fraction ratio between the $\Lambda_b^0 \rightarrow \eta_c p K^-$ and $\Lambda_b^0 \rightarrow J/\psi p K^-$ decays will provide the first comparison of b -baryon decay rates to the $\eta_c X$ and $J/\psi X$ final states, and help to test whether the presence of an additional spectator quark modifies the final-state interactions in a non-negligible way.

The LHCb detector is a single-arm forward spectrometer covering the pseudorapidity range $2 < \eta < 5$, and is described in detail in Refs. [31, 32]. The detector includes a silicon-strip vertex detector surrounding the proton-proton interaction region, tracking stations on either side of a dipole magnet, ring-imaging Cherenkov (RICH) detectors, calorimeters and muon chambers. The online event selection is performed by a trigger [33], which consists of a hardware stage, based on information from the calorimeter and muon systems, followed by a software stage, which applies a full event reconstruction. The software trigger requires a two-, three- or four-track secondary vertex with a significant displacement from any primary vertex (PV) that is consistent with originating from the decay of a b hadron [34].

Simulated data samples as described in Refs. [35–40], are used to optimize the event

selection, determine the efficiency of the reconstruction and event selection, and to constrain the fit model which determines the signal yield. The simulated $\Lambda_b^0 \rightarrow \eta_c p K^-$ and $\Lambda_b^0 \rightarrow J/\psi p K^-$ decays are generated based on a uniform phase-space model. The simulated decays are also weighted to match the Λ_b^0 momentum spectrum and Dalitz-plot distribution in the data, as described later in this paper.

The $\Lambda_b^0 \rightarrow \eta_c (\rightarrow p\bar{p}) p K^-$, and $\Lambda_b^0 \rightarrow J/\psi (\rightarrow p\bar{p}) p K^-$ candidates are reconstructed and selected using the same selection criteria, with a $p\bar{p}$ mass window of $[2800, 3200]$ MeV/ c^2 that covers both the η_c and J/ψ mass regions. In the following, the notation $[c\bar{c}]$ will be used to refer to both the η_c and the J/ψ candidates from Λ_b^0 baryon decays. Particle identification (PID) variables in the simulation are calibrated using large data samples of kinematically identified protons and kaons, originating from $\Lambda_b^0 \rightarrow \Lambda_c^+ (\rightarrow p K^- \pi^+) \pi^-$ and $D^0 \rightarrow K^- \pi^+$ decays.

The offline event selection is performed using a preselection, followed by a requirement on the response of a boosted decision tree (BDT) classifier [41, 42]. In the preselection, each track is required to be of good quality. Kaons and protons are both required to have $p_T > 300$ MeV/ c , where p_T is the component of the momentum transverse to the beam. Protons are also required to have a momentum larger than 10 GeV/ c^2 , such that the kaons and protons can be distinguished by the RICH detectors. The sum of the p_T of the proton and kaon from the Λ_b^0 baryon is required to be larger than 900 MeV/ c . The $[c\bar{c}]$ candidate is required to have a good-quality vertex.

The Λ_b^0 candidate must have a good-quality decay vertex that is significantly displaced from every PV, and have $\chi_{\text{IP}}^2 < 25$ with respect to the associated PV. Here, χ_{IP}^2 is defined as the χ^2 difference between the vertex fit of a PV reconstructed with or without the particle in question, and the associated PV is the one with the smallest χ_{IP}^2 value. The angle between the reconstructed momentum vector of the Λ_b^0 candidate and the line connecting the associated PV and the Λ_b^0 decay vertex, $\theta_{\Lambda_b^0}$, is required to satisfy $\cos(\theta_{\Lambda_b^0}) > 0.9999$.

Contamination from $B_s^0 \rightarrow p\bar{p}K^+K^-$ and $B^0 \rightarrow p\bar{p}K^+\pi^-$ decays, where a kaon or pion is misidentified as a proton, is removed by applying strict particle identification requirements on candidates with a mass within ± 50 MeV/ c^2 around the known B_s^0 or B^0 mass [30] after assigning a kaon or pion mass hypothesis to the proton. Backgrounds from $\phi(1020) \rightarrow K^+K^-$ and $D^0 \rightarrow K^+K^-$ decays, where one of the kaons is misidentified as a proton and the Λ_b^0 candidate is formed by combining the particles with a $[c\bar{c}]$ candidate from elsewhere in the event, are also observed. These contributions are removed by placing stricter particle-identification requirements on candidates with a pK^- mass within ± 10 MeV/ c^2 (± 20 MeV/ c^2) of the known $\phi(1020)$ (D^0) mass, after assigning a kaon mass hypothesis [30] to the proton.

After the preselection, further separation between the signal and combinatorial backgrounds originating from a random combination of final-state particles is achieved by using a BDT classifier. The classifier uses the following input variables: the p_T of the Λ_b^0 candidate, and of the kaon and proton directly from the Λ_b^0 decay; the χ_{IP}^2 of the Λ_b^0 candidate, the $[c\bar{c}]$ candidate, and the kaon and proton directly from the Λ_b^0 decay; the smallest values of both the p_T and χ_{IP}^2 of the $[c\bar{c}]$ decay products; the significance of the displacement of the Λ_b^0 vertex with respect to the associated PV; the vertex-fit χ^2 of the Λ_b^0 candidate; the $\theta_{\Lambda_b^0}$ angle; and the PID information of the final-state particles. The BDT is trained using simulated $\Lambda_b^0 \rightarrow \eta_c p K^-$ decays for the signal, and the data candidates in the $p\bar{p}pK^-$ invariant-mass sideband above 5800 MeV/ c^2 for the background. The requirement on the BDT response is optimized by maximizing the figure of merit

$\epsilon^{\text{sig}}/(a/2 + \sqrt{N_{\text{bkg}}})$ [43], where ϵ^{sig} is the BDT selection efficiency estimated using the simulated $\Lambda_b^0 \rightarrow \eta_c p K^-$ sample, $a = 5$ is the target significance for the signal in standard deviations, and N_{bkg} is the expected yield of background with $p\bar{p}$ and $p\bar{p}pK^-$ masses in the ranges $m(p\bar{p}) \in [2951.4, 3015.4] \text{ MeV}/c^2$ and $m(p\bar{p}pK^-) \in [5585, 5655] \text{ MeV}/c^2$, respectively. The background yields are estimated using the $p\bar{p}pK^-$ and $p\bar{p}$ invariant-mass sidebands in the data. The BDT response requirement provides about 70% signal efficiency and suppresses the background by a factor of approximately 100. After the BDT selection, a background in the normalization channel is observed due to swapping the proton from the Λ_b^0 decay with a proton from the J/ψ decay. This contribution is removed by requiring the invariant mass of the system formed by the proton from the Λ_b^0 baryon and the antiproton from the J/ψ meson to be inconsistent with the known J/ψ mass [30]. The $p\bar{p}pK^-$ and $p\bar{p}$ invariant-mass spectra of the selected data are displayed in Fig. 1.

A two-dimensional unbinned maximum-likelihood fit to the $p\bar{p}pK^-$ and $p\bar{p}$ invariant-mass distributions is performed to determine the signal yield. The $p\bar{p}pK^-$ mass spectra of the signal and normalization channels are described using the same model, sharing the shape parameters. The signal is modeled by the sum of two Crystal Ball (CB) functions [44] with common peak positions. The tail parameters of the CB functions are determined from simulation, while the mean and width of the Gaussian cores are freely varying in the fit to the data. The $p\bar{p}$ mass spectrum is described with a relativistic Breit–Wigner function [45] convolved with a Gaussian resolution function for the η_c , and is described with the sum of two CB functions with common peak positions for the J/ψ decay.

When modeling the $m(p\bar{p})$ spectrum, the correlation between $m(p\bar{p}pK^-)$ and $m(p\bar{p})$ needs to be taken into account. The width (peak) parameter of the resolution function of the signal channel, and the width (peak) parameters of the Gaussian cores for the normalization channel, are parameterized as second-order (first-order) polynomial functions of $m(p\bar{p}pK^-)$; the coefficients of these polynomial functions are calibrated using simulated samples.

For the two-dimensional mass spectrum of the background components, it is assumed that $m(p\bar{p}pK^-)$ and $m(p\bar{p})$ are uncorrelated, which is corroborated using the background-dominated data sample before the BDT selection is applied. For background from $\Lambda_b^0 \rightarrow p\bar{p}pK^-$ decays but with the $p\bar{p}$ pair not originating from a η_c or J/ψ resonance, the $m(p\bar{p})$ spectrum is described using an exponential function, and the $m(p\bar{p}pK^-)$ spectrum is described using the same model as the signal but the parameters of the distribution are allowed to take different values in the fit. For background with a $[c\bar{c}] \rightarrow p\bar{p}$ process but not from a Λ_b^0 decay, the $m(p\bar{p}pK^-)$ distribution is described using an exponential function, and the $m(p\bar{p})$ spectrum is modeled by Breit–Wigner functions that are each convolved with a separate Gaussian function to describe the η_c and J/ψ resonances. In the fit, a Gaussian constraint of $31.9 \pm 0.7 \text{ MeV}/c^2$ [30] is applied to the natural width of the η_c meson for both the signal and background components. For combinatorial backgrounds, both the $m(p\bar{p}pK^-)$ and $m(p\bar{p})$ spectra are described using exponential functions. The background shape due to swapping the two protons in the $\Lambda_b^0 \rightarrow \eta_c(\rightarrow p\bar{p})pK^-$ decay shares the same shape in $m(p\bar{p}pK^-)$ as the signal channel, while the $m(p\bar{p})$ shape, and the relative yield with respect to the signal component of the signal channel, are determined from simulation. Given the limited yield of $\Lambda_b^0 \rightarrow \eta_c p K^-$ decays expected in this data sample, the interference between the $\Lambda_b^0 \rightarrow \eta_c p K^-$ and nonresonant $\Lambda_b^0 \rightarrow p\bar{p}pK^-$ decays is not considered. An amplitude analysis of a larger data set is needed to have sensitivity

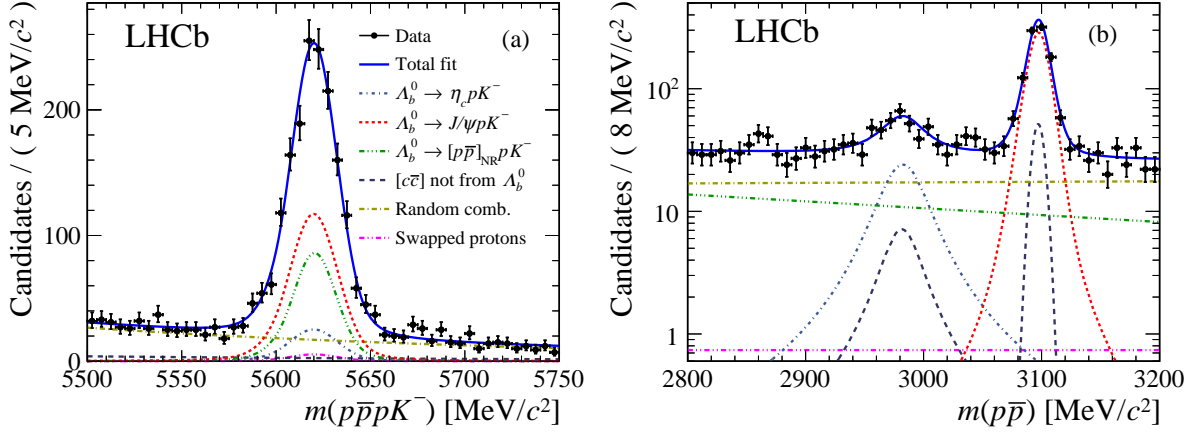


Figure 1: Distributions of (a) $m(p\bar{p}pK^-)$ and (b) $m(p\bar{p})$ of the selected candidates. The data are shown as black circles, while the blue solid line shows the fit result. Individual components are given in the legend.

to such interference effects.

The $m(p\bar{p}pK^-)$ and $m(p\bar{p})$ distributions of the selected candidates are presented in Fig. 1, with the one-dimensional projections of the fit overlaid. The yields of the signal and normalization modes are $N(\Lambda_b^0 \rightarrow \eta_c p K^-) = 173 \pm 25$ and $N(\Lambda_b^0 \rightarrow J/\psi p K^-) = 804 \pm 31$, respectively, where the uncertainties are statistical only. To estimate the signal significance, a two-dimensional fit without the contribution from the $\Lambda_b^0 \rightarrow \eta_c p K^-$ decay is performed. The difference in log-likelihood between this and the nominal fit is found to be 29.4. Based on the assumption of a χ^2 distribution with one degree of freedom, the statistical significance of the $\Lambda_b^0 \rightarrow \eta_c p K^-$ decay with respect to the background-only hypothesis, expressed in Gaussian standard deviations, is 7.7σ .

The ratio of the branching fraction between the $\Lambda_b^0 \rightarrow \eta_c p K^-$ and $\Lambda_b^0 \rightarrow J/\psi p K^-$ decays is given by

$$\frac{\mathcal{B}(\Lambda_b^0 \rightarrow \eta_c p K^-)}{\mathcal{B}(\Lambda_b^0 \rightarrow J/\psi p K^-)} = \frac{N(\Lambda_b^0 \rightarrow \eta_c p K^-)}{N(\Lambda_b^0 \rightarrow J/\psi p K^-)} \times \frac{\epsilon(\Lambda_b^0 \rightarrow J/\psi p K^-)}{\epsilon(\Lambda_b^0 \rightarrow \eta_c p K^-)} \times \frac{\mathcal{B}(J/\psi \rightarrow p\bar{p})}{\mathcal{B}(\eta_c \rightarrow p\bar{p})}, \quad (1)$$

where N represents the yield of the decay given in the parentheses, determined from a fit to the invariant-mass spectrum and ϵ is the efficiency accounting for the detector geometrical acceptance, reconstruction and event selection. The known values of the branching fractions, \mathcal{B} , of the $\Lambda_b^0 \rightarrow J/\psi p K^-$, $J/\psi \rightarrow p\bar{p}$ [30] and $\eta_c \rightarrow p\bar{p}$ decays [46] are used as external inputs for the measurement of $\mathcal{B}(\Lambda_b^0 \rightarrow \eta_c p K^-)$.

The efficiencies of the detector geometrical acceptance, reconstruction and event selections are determined from simulation. The agreement between data and simulation is improved by weighting the two-dimensional (p, p_T) distribution of the Λ_b^0 baryons in simulation. The weights are obtained using a comparison between a large sample of data and simulated events from $\Lambda_b^0 \rightarrow J/\psi p K^-$ decays, where the J/ψ meson is reconstructed through its decay $J/\psi \rightarrow \mu^+ \mu^-$. The distributions of $m(pK^-)$ and $m([c\bar{c}]p)$ in the simulation for signal and normalization channels are also weighted to match the corresponding distributions observed in data, where the data distributions are obtained using the *sPlot* technique [47] with $m(p\bar{p}pK^-)$ and $m(p\bar{p})$ as the discriminating variables. The ratio

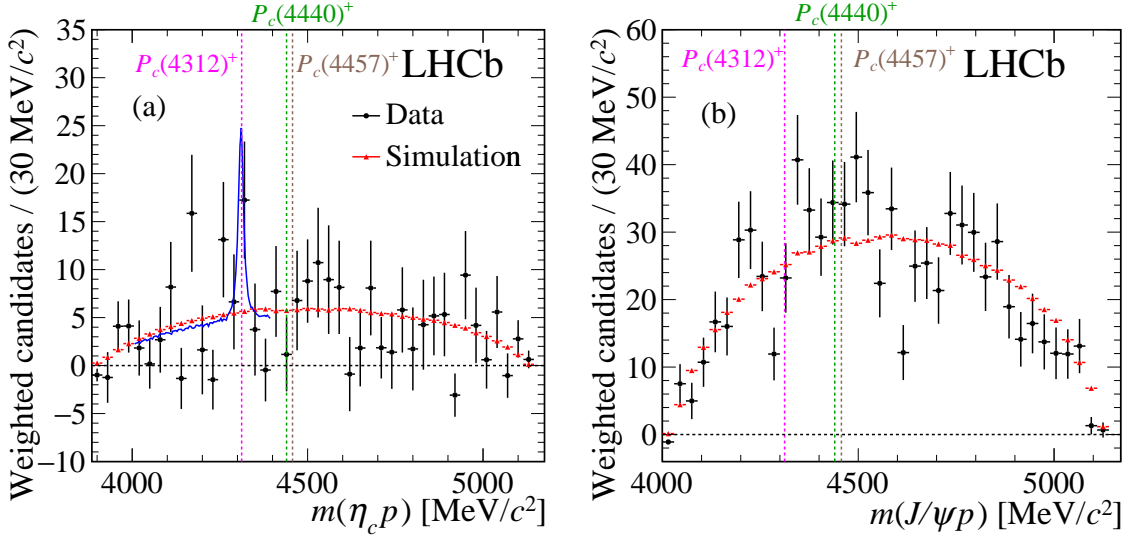


Figure 2: The invariant-mass spectra of (a) the $\eta_c p$ system of the $\Lambda_b^0 \rightarrow \eta_c p K^-$ decays and (b) the $J/\psi p$ system of the $\Lambda_b^0 \rightarrow J/\psi p K^-$ decays. The black points represent the background-subtracted data and the red points correspond to the expectation from a simulation generated according to a uniform phase-space model. The blue solid line in (a) shows the fit projection of the $\eta_c p$ mass spectrum including the contribution from a $P_c(4312)^+$ resonance in the mass range [4000, 4400] MeV/c².

between the overall efficiencies of the signal and normalization channels is 0.95 ± 0.02 , where the uncertainty accounts only for the finite yields of the simulated events. The ratio of branching fractions between the $\Lambda_b^0 \rightarrow \eta_c p K^-$ and $\Lambda_b^0 \rightarrow J/\psi p K^-$ decays is obtained as

$$\frac{\mathcal{B}(\Lambda_b^0 \rightarrow \eta_c p K^-)}{\mathcal{B}(\Lambda_b^0 \rightarrow J/\psi p K^-)} = 0.333 \pm 0.050,$$

where the quoted uncertainty is statistical only.

A search for a $P_c(4312)^+ \rightarrow \eta_c p$ contribution to the $\Lambda_b^0 \rightarrow \eta_c p K^-$ decay is performed by projecting out the background-subtracted $\eta_c p$ mass spectrum using the *sPlot* technique. The resulting $\eta_c p$ (and $J/\psi p$) mass distributions are shown in Fig. 2. A weighted unbinned maximum-likelihood fit [49] is applied to the $\eta_c p$ mass spectrum, where the data is described as the incoherent sum of $P_c(4312)^+ \rightarrow \eta_c p$ decays and a nonresonant $\eta_c p$ contribution. The $P_c(4312)^+$ resonance is modeled using a relativistic Breit–Wigner function [45], with parameters obtained from Ref. [5], and is convolved with the sum of two Gaussian resolution functions whose shape parameters are determined from simulation. The contribution from $\Lambda_b^0 \rightarrow \eta_c p K^-$ decays with a non-resonant $\eta_c p$ system is modeled using simulated events generated with a uniform phase-space model. The fit projection is shown in Fig. 2 (a).

The yield of the $P_c(4312)^+$ state is determined to be 16_{-9}^{+12} (stat.) ± 4 (syst.). The systematic uncertainty on the yield is estimated by using alternative models to describe the Λ_b^0 component without $\eta_c p$ resonances, and varying the mass and width of the $P_c(4312)^+$ state based on their uncertainties from Ref. [5]. To consider the potential influence of the interference between the $P_c(4312)^+$ component and reflections from $\Lambda^* \rightarrow p K^-$ resonances, several $\Lambda_b^0 \rightarrow J/\psi p K^-$ samples are generated based on the result of a full amplitude

fit to the $\Lambda_b^0 \rightarrow J/\psi (\rightarrow \mu^+ \mu^-) p K^-$ sample used in Ref. [5], with a different scale factor assigned on the $P_c(4312)^+$ amplitude to account for a change in its contribution. A fit is performed to these simulated $J/\psi p$ mass spectra, using the same description for the $P_c(4312)^+$ contribution as that in the fit model of the background-subtracted $\eta_c p$ mass spectrum. The largest relative difference between the $P_c(4312)^+$ relative contribution obtained from the fit and its true value in the simulated samples is taken as a systematic uncertainty for this potential interference.

The difference of the log-likelihood between the nominal fit and a fit with the $P_c(4312)^+$ yield fixed to zero is 2.4. Since all of the shape parameters of the $P_c(4312)^+$ component are fixed in the nominal fit, the statistical significance of the $P_c(4312)^+$ state is 2.2σ . Defining the relative $P_c(4312)^+$ contribution analogous to that which is used in Ref. [5] as

$$\mathcal{R} \equiv \frac{\mathcal{B}(\Lambda_b^0 \rightarrow P_c(4312)^+ K^-)}{\mathcal{B}(\Lambda_b^0 \rightarrow \eta_c p K^-)} \mathcal{B}(P_c(4312)^+ \rightarrow \eta_c p), \quad (2)$$

a 95% confidence level upper limit of $R < 0.24$ is obtained from the likelihood profile distribution. The search to the $P_c(4440)^+$ and $P_c(4457)^+$ states is not performed in this paper, as they will together perform like a broad structure under the limited sample size [4], which cannot be disentangled from the reflections from the $\Lambda_b^0 \rightarrow \Lambda^* \eta_c$, $\Lambda^* \rightarrow p K^-$ decay chain without a full amplitude analysis.

Sources of systematic uncertainty on the $\Lambda_b^0 \rightarrow \eta_c p K^-$ branching fraction arise from the fitting procedure and limited knowledge of the efficiencies, and are summarized in Table 1. Pseudoexperiments are used to estimate the effects due to parameters determined from simulation. Systematic uncertainties on the fit model are evaluated by using alternative fit models where: the exponential functions are replaced by Chebyshev polynomials; the contributions from genuine Λ_b^0 decays in the $m(p\bar{p}pK^-)$ spectrum are modeled by the Hypatia distribution [48]; the resolution of the η_c peaking structure in the $m(p\bar{p})$ spectrum is replaced by the average resolution of the CB functions describing the J/ψ peak; the shape parameters of the Λ_b^0 peak in the $\Lambda_b^0 \rightarrow p\bar{p}pK^-$ decay without the η_c or J/ψ resonances are fixed to be the same as those of the signal and the normalization decays. Pseudoexperiments are used to estimate the potential bias of the fit yields, which is found to be negligible compared to the statistical uncertainties. Based on each alternative fit model described above, the significance of the $\Lambda_b^0 \rightarrow \eta_c p K^-$ is reestimated. The smallest significance found is approximately 7.7σ . This is the first observation of this decay mode.

Uncertainties on the efficiency ratio between the signal and normalization channels are largely canceled due to the similarity of these two decay modes. For the estimation of systematic uncertainties related to the weighting procedure of $m([c\bar{c}]p)$, $m(pK^-)$ and (p, p_T) of the Λ_b^0 decays in simulation, pseudoexperiments are used to propagate the uncertainties of single-event weights, originating from the finite yield of the samples used to obtain the weights, to the uncertainty of the overall efficiency ratio; an alternative binning scheme is used to estimate the uncertainty due to the choice of binning in the weighting procedure; and the negative weights, given by the *sPlot* technique due to statistical fluctuations, are set to zero to recalculate the overall efficiency ratio. A systematic uncertainty is also assigned for the finite size of the simulated samples used for the efficiency estimation.

The total systematic uncertainty of the $\Lambda_b^0 \rightarrow \eta_c p K^-$ branching fraction measurement is obtained by adding the above contributions in quadrature, leading to a value of 5.8%, and details are given in Table 1. The dominant contribution is the uncertainty related

to the fit model. The limited knowledge of the branching fractions of the $\Lambda_b^0 \rightarrow J/\psi pK^-$, $J/\psi \rightarrow p\bar{p}$ and $\eta_c \rightarrow p\bar{p}$ decays [30] is also considered as an external source that contributes to the total uncertainty.

The background-subtracted data distributions of $m([c\bar{c}]p)$ for the signal and normalization channels are shown in Fig. 2, with the distributions of simulated events overlaid. The background subtraction is based on the *sPlot* technique [47], with $m(p\bar{p}pK^-)$ and $m(p\bar{p})$ as the discriminating variables. No significant peaking structures are seen. The fractions of the $P_c(4312)^+$, $P_c(4440)^+$ and $P_c(4457)^+$ contributions to the $\Lambda_b^0 \rightarrow J/\psi pK^-$ decays are only roughly 0.3%, 1.1% and 0.5%, respectively [5], and given the limited $\Lambda_b^0 \rightarrow J/\psi pK^-$ yields of this analysis, it is not surprising that these P_c contributions are not observed.

In summary, the first observation of the decay $\Lambda_b^0 \rightarrow \eta_c pK^-$ has been reported using proton-proton collision data collected with the LHCb experiment, corresponding to an integrated luminosity of 5.5 fb^{-1} . The significance of this observation, over the background-only hypothesis, is 7.7 standard deviations. The branching fraction ratio between the $\Lambda_b^0 \rightarrow \eta_c pK^-$ and $\Lambda_b^0 \rightarrow J/\psi pK^-$ decays is measured to be

$$\frac{\mathcal{B}(\Lambda_b^0 \rightarrow \eta_c pK^-)}{\mathcal{B}(\Lambda_b^0 \rightarrow J/\psi pK^-)} = 0.333 \pm 0.050 \text{ (stat.)} \pm 0.019 \text{ (syst.)} \pm 0.032 \text{ (}\mathcal{B}\text{)},$$

where the first uncertainty is statistical, the second is systematic, and the last is due to the uncertainty on the branching fractions of the $\eta_c \rightarrow p\bar{p}$ and $J/\psi \rightarrow p\bar{p}$ decays. Using this ratio, the branching fraction of the $\Lambda_b^0 \rightarrow \eta_c pK^-$ decay is determined to be

$$\mathcal{B}(\Lambda_b^0 \rightarrow \eta_c pK^-) = (1.06 \pm 0.16 \text{ (stat.)} \pm 0.06 \text{ (syst.)}_{-0.19}^{+0.22} \text{ (}\mathcal{B}\text{)}) \times 10^{-4},$$

where the third uncertainty also depends on the branching fraction of the $\Lambda_b^0 \rightarrow J/\psi pK^-$ decay.

The observation of this decay opens up a new line of investigation in searching for pentaquarks in the $\eta_c p$ system. If the $P_c(4312)^+$ state is a $\bar{D}\Sigma_c$ molecule and the predictions of Refs. [13–15] are accurate, a value of $R_{\bar{D}\Sigma_c} \sim 0.03$ would be expected, based on the $P_c(4312)^+$ relative contribution in $\Lambda_b^0 \rightarrow J/\psi pK^-$ decays [5] and the above result for $\mathcal{B}(\Lambda_b^0 \rightarrow \eta_c pK^-)/\mathcal{B}(\Lambda_b^0 \rightarrow J/\psi pK^-)$. The 95% confidence level upper limit obtained in this analysis, $R < 0.24$, does not exclude this molecular interpretation for the $P_c(4312)^+$

Table 1: Summary of the uncertainties on the branching fraction ratio $\mathcal{B}(\Lambda_b^0 \rightarrow \eta_c pK^-)/\mathcal{B}(\Lambda_b^0 \rightarrow J/\psi pK^-)$. The total systematic uncertainty is obtained by summing the individual contributions in quadrature.

Source	Uncertainty (%)
Λ_b^0 p and p_T distributions	1.0
$m(pK^-)$ and $m([c\bar{c}]p)$ distributions	3.2
Fit model	4.0
Finite simulated sample sizes	2.5
Total systematic uncertainty	5.8
Statistical uncertainty	13.6
$\mathcal{B}([c\bar{c}] \rightarrow p\bar{p})$	9.6

state. A further amplitude analysis with a larger data sample is required for a more quantitative comparison to theoretical predictions [13–15]. By using an upgraded LHCb detector with improved trigger conditions and larger data samples collected, there are good prospects for using this decay to shed light on the binding mechanism of the recently observed pentaquark states [5].

Acknowledgements

We express our gratitude to our colleagues in the CERN accelerator departments for the excellent performance of the LHC. We thank the technical and administrative staff at the LHCb institutes. We acknowledge support from CERN and from the national agencies: CAPES, CNPq, FAPERJ and FINEP (Brazil); MOST and NSFC (China); CNRS/IN2P3 (France); BMBF, DFG and MPG (Germany); INFN (Italy); NWO (Netherlands); MNiSW and NCN (Poland); MEN/IFA (Romania); MSHE (Russia); MICINN (Spain); SNSF and SER (Switzerland); NASU (Ukraine); STFC (United Kingdom); DOE NP and NSF (USA). We acknowledge the computing resources that are provided by CERN, IN2P3 (France), KIT and DESY (Germany), INFN (Italy), SURF (Netherlands), PIC (Spain), GridPP (United Kingdom), RRCKI and Yandex LLC (Russia), CSCS (Switzerland), IFIN-HH (Romania), CBPF (Brazil), PL-GRID (Poland) and OSC (USA). We are indebted to the communities behind the multiple open-source software packages on which we depend. Individual groups or members have received support from AvH Foundation (Germany); EPLANET, Marie Skłodowska-Curie Actions and ERC (European Union); A*MIDEX, ANR, Labex P2IO and OCEVU, and Région Auvergne-Rhône-Alpes (France); Key Research Program of Frontier Sciences of CAS, CAS PIFI, Thousand Talents Program, and Sci. & Tech. Program of Guangzhou (China); RFBR, RSF and Yandex LLC (Russia); GVA, XuntaGal and GENCAT (Spain); the Royal Society and the Leverhulme Trust (United Kingdom).

References

- [1] M. Gell-Mann, *A schematic model of baryons and mesons*, Phys. Lett. **8** (1964) 214.
- [2] G. Zweig, *An SU_3 model for strong interaction symmetry and its breaking; Version 2*, CERN-TH-412, CERN, Geneva, 1964.
- [3] H. J. Lipkin, *New possibilities for exotic hadrons – anticharmed strange baryons*, Phys. Lett. **B195** (1987) 484.
- [4] LHCb collaboration, R. Aaij *et al.*, *Observation of $J/\psi p$ resonances consistent with pentaquark states in $\Lambda_b^0 \rightarrow J/\psi p K^-$ decays*, Phys. Rev. Lett. **115** (2015) 072001, arXiv:1507.03414.
- [5] LHCb collaboration, R. Aaij *et al.*, *Observation of a narrow pentaquark state, $P_c(4312)^+$, and of two-peak structure of the $P_c(4450)^+$* , Phys. Rev. Lett. **122** (2019) 222001, arXiv:1904.03947.
- [6] L. Maiani, A. D. Polosa, and V. Riquer, *The new pentaquarks in the diquark model*, Phys. Lett. **B749** (2015) 289, arXiv:1507.04980.
- [7] R. F. Lebed, *The pentaquark candidates in the dynamical diquark picture*, Phys. Lett. **B749** (2015) 454, arXiv:1507.05867.
- [8] V. V. Anisovich *et al.*, *Pentaquarks and resonances in the pJ/ψ spectrum*, arXiv:1507.07652.
- [9] G.-N. Li, X.-G. He, and M. He, *Some predictions of diquark model for hidden charm pentaquark discovered at the LHCb*, JHEP **12** (2015) 128, arXiv:1507.08252.
- [10] R. Ghosh, A. Bhattacharya, and B. Chakrabarti, *A study on $P_c^*(4380)$ and P_c^* in the quasi particle diquark model*, Phys. Part. Nucl. Lett. **14** (2017) 550, arXiv:1508.00356.
- [11] Z.-G. Wang, *Analysis of $P_c(4380)$ and $P_c(4450)$ as pentaquark states in the diquark model with QCD sum rules*, Eur. Phys. J. **C76** (2016) 70, arXiv:1508.01468.
- [12] R. Zhu and C.-F. Qiao, *Pentaquark states in a diquark-triquark model*, Phys. Lett. **B756** (2016) 259, arXiv:1510.08693.
- [13] M. B. Voloshin, *Some decay properties of hidden-charm pentaquarks as baryon-meson molecules*, Phys. Rev. **D100** (2019) 034020, arXiv:1907.01476.
- [14] S. Sakai, H.-J. Jing, and F.-K. Guo, *Decays of P_c into $J/\psi N$ and $\eta_c N$ with heavy quark spin symmetry*, Phys. Rev. **D100** (2019) 074007, arXiv:1907.03414.
- [15] G.-J. Wang *et al.*, *Probing hidden-charm decay properties of P_c states in a molecular scenario*, Phys. Rev. D **102** (2020) 036012, arXiv:1911.09613.
- [16] M. Karliner and J. L. Rosner, *New exotic meson and baryon resonances from doubly-heavy hadronic molecules*, Phys. Rev. Lett. **115** (2015) 122001, arXiv:1506.06386.

- [17] R. Chen, X. Liu, X.-Q. Li, and S.-L. Zhu, *Identifying exotic hidden-charm pentaquarks*, Phys. Rev. Lett. **115** (2015) 132002, arXiv:1507.03704.
- [18] H.-X. Chen *et al.*, *Towards exotic hidden-charm pentaquarks in QCD*, Phys. Rev. Lett. **115** (2015) 172001, arXiv:1507.03717.
- [19] L. Roca, J. Nieves, and E. Oset, *LHCb pentaquark as a $\bar{D}^*\Sigma_c - \bar{D}^*\Sigma_c^*$ molecular state*, Phys. Rev. **D92** (2015) 094003, arXiv:1507.04249.
- [20] J. He, *$\bar{D}\Sigma_c^*$ and $\bar{D}^*\Sigma_c$ interactions and the LHCb hidden-charmed pentaquarks*, Phys. Lett. **B753** (2016) 547, arXiv:1507.05200.
- [21] H. Huang, C. Deng, J. Ping, and F. Wang, *Possible pentaquarks with heavy quarks*, Eur. Phys. J. **C76** (2016) 624, arXiv:1510.04648.
- [22] F.-K. Guo, U.-G. Meißner, W. Wang, and Z. Yang, *How to reveal the exotic nature of the $P_c(4450)$* , Phys. Rev. **D92** (2015) 071502, arXiv:1507.04950.
- [23] U.-G. Meißner and J. A. Oller, *Testing the $\chi_{c1}p$ composite nature of the $P_c(4450)$* , Phys. Lett. **B751** (2015) 59, arXiv:1507.07478.
- [24] X.-H. Liu, Q. Wang, and Q. Zhao, *Understanding the newly observed heavy pentaquark candidates*, Phys. Lett. **B757** (2016) 231, arXiv:1507.05359.
- [25] M. Mikhasenko, *A triangle singularity and the LHCb pentaquarks*, arXiv:1507.06552.
- [26] J.-J. Xie, W.-H. Liang, and E. Oset, *Hidden charm pentaquark and $\Lambda(1405)$ in the $\Lambda_b^0 \rightarrow \eta_c K^- p(\pi\Sigma)$ reaction*, Phys. Lett. **B777** (2018) 447, arXiv:1711.01710.
- [27] J.-J. Wu, T.-S. H. Lee, and B.-S. Zou, *Nucleon resonances with hidden charm in $p\gamma$ reactions*, Phys. Rev. **C100** (2019) 035206, arXiv:1906.05375.
- [28] N. G. Deshpande and J. Trampetic, *Exclusive and semi-inclusive B decays based on $b \rightarrow s\eta_c$ transition*, Phys. Lett. **B339** (1994) 270, arXiv:hep-ph/9406393.
- [29] M. R. Ahmady and R. R. Mendel, *A theoretical prediction for exclusive decays $B \rightarrow K(K^*)\eta_c$* , Z. Phys. **C65** (1995) 263, arXiv:hep-ph/9401327.
- [30] Particle Data Group, M. Tanabashi *et al.*, *Review of particle physics*, Phys. Rev. **D98** (2018) 030001, and 2019 update.
- [31] LHCb collaboration, A. A. Alves, Jr. *et al.*, *The LHCb detector at the LHC*, JINST **3** (2008) S08005.
- [32] LHCb collaboration, R. Aaij *et al.*, *LHCb detector performance*, Int. J. Mod. Phys. **A30** (2015) 1530022, arXiv:1412.6352.
- [33] R. Aaij *et al.*, *Performance of the LHCb trigger and full real-time reconstruction in Run 2 of the LHC*, JINST **14** (2019) P04013, arXiv:1812.10790.
- [34] V. V. Gligorov and M. Williams, *Efficient, reliable and fast high-level triggering using a bonsai boosted decision tree*, JINST **8** (2013) P02013, arXiv:1210.6861.

- [35] T. Sjöstrand, S. Mrenna, and P. Skands, *A brief introduction to PYTHIA 8.1*, Comput. Phys. Commun. **178** (2008) 852, [arXiv:0710.3820](#).
- [36] I. Belyaev *et al.*, *Handling of the generation of primary events in Gauss, the LHCb simulation framework*, J. Phys. Conf. Ser. **331** (2011) 032047.
- [37] D. J. Lange, *The EvtGen particle decay simulation package*, Nucl. Instrum. Meth. **A462** (2001) 152.
- [38] P. Golonka and Z. Was, *PHOTOS Monte Carlo: A precision tool for QED corrections in Z and W decays*, Eur. Phys. J. **C45** (2006) 97, [arXiv:hep-ph/0506026](#).
- [39] Geant4 collaboration, J. Allison *et al.*, *Geant4 developments and applications*, IEEE Trans. Nucl. Sci. **53** (2006) 270.
- [40] M. Clemencic *et al.*, *The LHCb simulation application, Gauss: design, evolution and experience*, J. Phys. Conf. Ser. **331** (2011) 032023.
- [41] Y. Freund and R. E. Schapire, *A decision-theoretic generalization of on-line learning and an application to boosting*, Journal of Computer and System Sciences **55** (1997) 119 .
- [42] H. Voss, A. Hoecker, J. Stelzer, and F. Tegenfeldt, *TMVA, The toolkit for Multivariate Data Analysis with ROOT*, PoS **ACAT** (2007) 040.
- [43] G. Punzi, *Sensitivity of searches for new signals and its optimization*, eConf **C030908** (2003) MODT002, [arXiv:physics/0308063](#).
- [44] T. Skwarnicki, *A study of the radiative cascade transitions between the Upsilon-prime and Upsilon resonances*, PhD thesis, Institute of Nuclear Physics, Krakow, 1986, DESY-F31-86-02.
- [45] J. D. Jackson, *Remarks on the phenomenological analysis of resonances*, Nuovo Cim. **34** (1964) 1644.
- [46] Particle Data Group, P. A. Zyla *et al.*, *Review of particle physics*, to be published in Prog. Theor. Exp. Phys. **2020** (2020) 083C01.
- [47] M. Pivk and F. R. Le Diberder, *sPlot: A statistical tool to unfold data distributions*, Nucl. Instrum. Meth. **A555** (2005) 356, [arXiv:physics/0402083](#).
- [48] D. Martínez Santos and F. Dupertuis, *Mass distributions marginalized over per-event errors*, Nucl. Instrum. Meth. **A764** (2014) 150, [arXiv:1312.5000](#).
- [49] Y. Xie, *sFit: a method for background subtraction in maximum likelihood fit*, [arXiv:0905.0724](#).

LHCb collaboration

R. Aaij³¹, C. Abellán Beteta⁴⁹, T. Ackernley⁵⁹, B. Adeva⁴⁵, M. Adinolfi⁵³, H. Afsharnia⁹, C.A. Aidala⁸³, S. Aiola²⁵, Z. Ajaltouni⁹, S. Akar⁶⁴, J. Albrecht¹⁴, F. Alessio⁴⁷, M. Alexander⁵⁸, A. Alfonso Alberro⁴⁴, Z. Aliouche⁶¹, G. Alkhazov³⁷, P. Alvarez Cartelle⁴⁷, A.A. Alves Jr⁴⁵, S. Amato², Y. Amhis¹¹, L. An²¹, L. Anderlini²¹, G. Andreassi⁴⁸, A. Andreianov³⁷, M. Andreotti²⁰, F. Archilli¹⁶, A. Artamonov⁴³, M. Artuso⁶⁷, K. Arzymatov⁴¹, E. Aslanides¹⁰, M. Atzeni⁴⁹, B. Audurier¹¹, S. Bachmann¹⁶, M. Bachmayer⁴⁸, J.J. Back⁵⁵, S. Baker⁶⁰, P. Baladron Rodriguez⁴⁵, V. Balagura^{11,b}, W. Baldini²⁰, J. Baptista Leite¹, R.J. Barlow⁶¹, S. Barsuk¹¹, W. Barter⁶⁰, M. Bartolini^{23,47,i}, F. Baryshnikov⁸⁰, J.M. Basels¹³, G. Bassi²⁸, V. Batozskaya³⁵, B. Batsukh⁶⁷, A. Battig¹⁴, A. Bay⁴⁸, M. Becker¹⁴, F. Bedeschi²⁸, I. Bediaga¹, A. Beiter⁶⁷, V. Belavin⁴¹, S. Belin²⁶, V. Bellee⁴⁸, K. Belous⁴³, I. Belov³⁹, I. Belyaev³⁸, G. Bencivenni²², E. Ben-Haim¹², A. Berezhnoy³⁹, R. Bernet⁴⁹, D. Berninghoff¹⁶, H.C. Bernstein⁶⁷, C. Bertella⁴⁷, E. Bertholet¹², A. Bertolin²⁷, C. Betancourt⁴⁹, F. Betti^{19,e}, M.O. Bettler⁵⁴, I.a. Bezshyiko⁴⁹, S. Bhasin⁵³, J. Bhom³³, L. Bian⁷², M.S. Bieker¹⁴, S. Bifani⁵², P. Billoir¹², M. Birch⁶⁰, F.C.R. Bishop⁵⁴, A. Bizzeti^{21,u}, M. Bjørn⁶², M.P. Blago⁴⁷, T. Blake⁵⁵, F. Blanc⁴⁸, S. Blusk⁶⁷, D. Bobulska⁵⁸, V. Bocci³⁰, J.A. Boelhauve¹⁴, O. Boente Garcia⁴⁵, T. Boettcher⁶³, A. Boldyrev⁸¹, A. Bondar^{42,x}, N. Bondar^{37,47}, S. Borghi⁶¹, M. Borisyak⁴¹, M. Borsato¹⁶, J.T. Borsuk³³, S.A. Bouchiba⁴⁸, T.J.V. Bowcock⁵⁹, A. Boyer⁴⁷, C. Bozzi²⁰, M.J. Bradley⁶⁰, S. Braun⁶⁵, A. Brea Rodriguez⁴⁵, M. Brodski⁴⁷, J. Brodzicka³³, A. Brossa Gonzalo⁵⁵, D. Brundu²⁶, A. Buonauro⁴⁹, C. Burr⁴⁷, A. Bursche²⁶, A. Butkevich⁴⁰, J.S. Butter³¹, J. Buytaert⁴⁷, W. Byczynski⁴⁷, S. Cadeddu²⁶, H. Cai⁷², R. Calabrese^{20,g}, L. Calefice¹⁴, L. Calero Diaz²², S. Cali²², R. Calladine⁵², M. Calvi^{24,j}, M. Calvo Gomez^{44,m}, P. Camargo Magalhaes⁵³, A. Camboni⁴⁴, P. Campana²², D.H. Campora Perez⁴⁷, A.F. Campoverde Quezada⁵, S. Capelli^{24,j}, L. Capriotti^{19,e}, A. Carbone^{19,e}, G. Carboni²⁹, R. Cardinale^{23,i}, A. Cardini²⁶, I. Carli⁶, P. Carniti^{24,j}, K. Carvalho Akiba³¹, A. Casais Vidal⁴⁵, G. Casse⁵⁹, M. Cattaneo⁴⁷, G. Cavallero⁴⁷, S. Celani⁴⁸, R. Cenci²⁸, J. Cerasoli¹⁰, A.J. Chadwick⁵⁹, M.G. Chapman⁵³, M. Charles¹², Ph. Charpentier⁴⁷, G. Chatzikonstantinidis⁵², C.A. Chavez Barajas⁵⁹, M. Chefdeville⁸, C. Chen³, S. Chen²⁶, A. Chernov³³, S.-G. Chitic⁴⁷, V. Chobanova⁴⁵, S. Cholak⁴⁸, M. Chruszacz³³, A. Chubykin³⁷, V. Chulikov³⁷, P. Ciambrone²², M.F. Cicala⁵⁵, X. Cid Vidal⁴⁵, G. Ciezarek⁴⁷, P.E.L. Clarke⁵⁷, M. Clemencic⁴⁷, H.V. Cliff⁵⁴, J. Closier⁴⁷, J.L. Cobbledick⁶¹, V. Coco⁴⁷, J.A.B. Coelho¹¹, J. Cogan¹⁰, E. Cogneras⁹, L. Cojocariu³⁶, P. Collins⁴⁷, T. Colombo⁴⁷, L. Congedo¹⁸, A. Contu²⁶, N. Cooke⁵², G. Coombs⁵⁸, S. Coquereau⁴⁴, G. Corti⁴⁷, C.M. Costa Sobral⁵⁵, B. Couturier⁴⁷, D.C. Craik⁶³, J. Crkovská⁶⁶, M. Cruz Torres^{1,z}, R. Currie⁵⁷, C.L. Da Silva⁶⁶, E. Dall’Occo¹⁴, J. Dalseno⁴⁵, C. D’Ambrosio⁴⁷, A. Danilina³⁸, P. d’Argent⁴⁷, A. Davis⁶¹, O. De Aguiar Francisco⁴⁷, K. De Bruyn⁴⁷, S. De Capua⁶¹, M. De Cian⁴⁸, J.M. De Miranda¹, L. De Paula², M. De Serio^{18,d}, D. De Simone⁴⁹, P. De Simone²², J.A. de Vries⁷⁸, C.T. Dean⁶⁶, W. Dean⁸³, D. Decamp⁸, L. Del Buono¹², B. Delaney⁵⁴, H.-P. Dembinski¹⁴, A. Dendek³⁴, V. Denysenko⁴⁹, D. Derkach⁸¹, O. Deschamps⁹, F. Desse¹¹, F. Dettori^{26,f}, B. Dey⁷, P. Di Nezza²², S. Didenko⁸⁰, L. Dieste Maronas⁴⁵, H. Dijkstra⁴⁷, V. Dobishuk⁵¹, A.M. Donohoe¹⁷, F. Dordei²⁶, M. Dorigo^{28,y}, A.C. dos Reis¹, L. Douglas⁵⁸, A. Dovbnya⁵⁰, A.G. Downes⁸, K. Dreimanis⁵⁹, M.W. Dudek³³, L. Dufour⁴⁷, V. Duk⁷⁶, P. Durante⁴⁷, J.M. Durham⁶⁶, D. Dutta⁶¹, M. Dziewiecki¹⁶, A. Dziurda³³, A. Dzyuba³⁷, S. Easo⁵⁶, U. Egede⁶⁹, V. Egorychev³⁸, S. Eidelman^{42,x}, S. Eisenhardt⁵⁷, S. Ek-In⁴⁸, L. Eklund⁵⁸, S. Ely⁶⁷, A. Ene³⁶, E. Epple⁶⁶, S. Escher¹³, J. Eschle⁴⁹, S. Esen³¹, T. Evans⁴⁷, A. Falabella¹⁹, J. Fan³, Y. Fan⁵, B. Fang⁷², N. Farley⁵², S. Farry⁵⁹, D. Fazzini¹¹, P. Fedin³⁸, M. Féo⁴⁷, P. Fernandez Declara⁴⁷, A. Fernandez Prieto⁴⁵, F. Ferrari^{19,e}, L. Ferreira Lopes⁴⁸, F. Ferreira Rodrigues², S. Ferreres Sole³¹, M. Ferrillo⁴⁹, M. Ferro-Luzzi⁴⁷, S. Filippov⁴⁰, R.A. Fini¹⁸, M. Fiorini^{20,g}, M. Firlej³⁴, K.M. Fischer⁶², C. Fitzpatrick⁶¹, T. Fiutowski³⁴, F. Fleuret^{11,b}, M. Fontana⁴⁷, F. Fontanelli^{23,i}, R. Forty⁴⁷, V. Franco Lima⁵⁹,

M. Franco Sevilla⁶⁵, M. Frank⁴⁷, E. Franzoso²⁰, G. Frau¹⁶, C. Frei⁴⁷, D.A. Friday⁵⁸, J. Fu^{25,q},
Q. Fuehring¹⁴, W. Funk⁴⁷, E. Gabriel³¹, T. Gaintseva⁴¹, A. Gallas Torreira⁴⁵, D. Galli^{19,e},
S. Gallorini²⁷, S. Gambetta⁵⁷, Y. Gan³, M. Gandelman², P. Gandini²⁵, Y. Gao⁴, M. Garau²⁶,
L.M. Garcia Martin⁴⁶, P. Garcia Moreno⁴⁴, J. García Pardiñas⁴⁹, B. Garcia Plana⁴⁵,
F.A. Garcia Rosales¹¹, L. Garrido⁴⁴, D. Gascon⁴⁴, C. Gaspar⁴⁷, R.E. Geertsema³¹, D. Gerick¹⁶,
L.L. Gerken¹⁴, E. Gersabeck⁶¹, M. Gersabeck⁶¹, T. Gershon⁵⁵, D. Gerstel¹⁰, Ph. Ghez⁸,
V. Gibson⁵⁴, M. Giovannetti^{22,k}, A. Gioventù⁴⁵, P. Gironella Gironell⁴⁴, L. Giubega³⁶,
C. Giugliano^{20,g}, K. Gizdov⁵⁷, E.L. Gkougkousis⁴⁷, V.V. Gligorov¹², C. Göbel⁷⁰,
E. Golobardes^{44,m}, D. Golubkov³⁸, A. Golutvin^{60,80}, A. Gomes^{1,a}, S. Gomez Fernandez⁴⁴,
M. Goncerz³³, G. Gong³, P. Gorbounov³⁸, I.V. Gorelov³⁹, C. Gotti^{24,j}, E. Govorkova³¹,
J.P. Grabowski¹⁶, R. Graciani Diaz⁴⁴, T. Grammatico¹², L.A. Granado Cardoso⁴⁷,
E. Graugés⁴⁴, E. Graverini⁴⁸, G. Graziani²¹, A. Grecu³⁶, L.M. Greeven³¹, P. Griffith²⁰,
L. Grillo⁶¹, S. Gromov⁸⁰, L. Gruber⁴⁷, B.R. Gruber Cazon⁶², C. Gu³, M. Guarise²⁰, P.
A. Günther¹⁶, E. Gushchin⁴⁰, A. Guth¹³, Y. Guz^{43,47}, T. Gys⁴⁷, T. Hadavizadeh⁶⁹, G. Haefeli⁴⁸,
C. Haen⁴⁷, J. Haimberger⁴⁷, S.C. Haines⁵⁴, T. Halewood-leagas⁵⁹, P.M. Hamilton⁶⁵, Q. Han⁷,
X. Han¹⁶, T.H. Hancock⁶², S. Hansmann-Menzemer¹⁶, N. Harnew⁶², T. Harrison⁵⁹, R. Hart³¹,
C. Hasse⁴⁷, M. Hatch⁴⁷, J. He⁵, M. Hecker⁶⁰, K. Heijhoff³¹, K. Heinicke¹⁴, A.M. Hennequin⁴⁷,
K. Hennessy⁵⁹, L. Henry^{25,46}, J. Heuel¹³, A. Hicheur⁶⁸, D. Hill⁶², M. Hilton⁶¹, S.E. Hollitt¹⁴,
P.H. Hopchev⁴⁸, J. Hu¹⁶, J. Hu⁷¹, W. Hu⁷, W. Huang⁵, X. Huang⁷², W. Hulsbergen³¹,
T. Humair⁶⁰, R.J. Hunter⁵⁵, M. Hushchyn⁸¹, D. Hutchcroft⁵⁹, D. Hynds³¹, P. Ibis¹⁴, M. Idzik³⁴,
D. Ilin³⁷, P. Ilten⁵², A. Inglessi³⁷, A. Ishteev⁸⁰, K. Ivshin³⁷, R. Jacobsson⁴⁷, S. Jakobsen⁴⁷,
E. Jans³¹, B.K. Jashal⁴⁶, A. Jawahery⁶⁵, V. Jevtic¹⁴, M. Jezabek³³, F. Jiang³, M. John⁶²,
D. Johnson⁴⁷, C.R. Jones⁵⁴, T.P. Jones⁵⁵, B. Jost⁴⁷, N. Jurik⁶², S. Kandybei⁵⁰, Y. Kang³,
M. Karacson⁴⁷, J.M. Kariuki⁵³, N. Kazeev⁸¹, M. Kecke¹⁶, F. Keizer^{54,47}, M. Kelsey⁶⁷,
M. Kenzie⁵⁵, T. Ketel³², B. Khanji⁴⁷, A. Kharisova⁸², S. Kholodenko⁴³, K.E. Kim⁶⁷, T. Kirn¹³,
V.S. Kirsebom⁴⁸, O. Kitouni⁶³, S. Klaver³¹, K. Klimaszewski³⁵, S. Koliiev⁵¹, A. Kondybayeva⁸⁰,
A. Konoplyannikov³⁸, P. Kopciwicz³⁴, R. Kopecna¹⁶, P. Koppenburg³¹, M. Korolev³⁹,
I. Kostiuik^{31,51}, O. Kot⁵¹, S. Kotriakhova^{37,30}, P. Kravchenko³⁷, L. Kravchuk⁴⁰,
R.D. Krawczyk⁴⁷, M. Kreps⁵⁵, F. Kress⁶⁰, S. Kretzschmar¹³, P. Krokovny^{42,x}, W. Krupa³⁴,
W. Krzemien³⁵, W. Kucewicz^{33,l}, M. Kucharczyk³³, V. Kudryavtsev^{42,x}, H.S. Kuindersma³¹,
G.J. Kunde⁶⁶, T. Kvaratskheliya³⁸, D. Lacarrere⁴⁷, G. Lafferty⁶¹, A. Lai²⁶, A. Lampis²⁶,
D. Lancierini⁴⁹, J.J. Lane⁶¹, R. Lane⁵³, G. Lanfranchi²², C. Langenbruch¹³, J. Langer¹⁴,
O. Lantwin^{49,80}, T. Latham⁵⁵, F. Lazzari^{28,v}, R. Le Gac¹⁰, S.H. Lee⁸³, R. Lefèvre⁹,
A. Leflat^{39,47}, S. Legotin⁸⁰, O. Leroy¹⁰, T. Lesiak³³, B. Leverington¹⁶, H. Li⁷¹, L. Li⁶², P. Li¹⁶,
X. Li⁶⁶, Y. Li⁶, Y. Li⁶, Z. Li⁶⁷, X. Liang⁶⁷, T. Lin⁶⁰, R. Lindner⁴⁷, V. Lisovskyi¹⁴, R. Litvinov²⁶,
G. Liu⁷¹, H. Liu⁵, S. Liu⁶, X. Liu³, A. Loi²⁶, J. Lomba Castro⁴⁵, I. Longstaff⁵⁸, J.H. Lopes²,
G. Loustau⁴⁹, G.H. Lovell⁵⁴, Y. Lu⁶, D. Lucchesi^{27,o}, S. Luchuk⁴⁰, M. Lucio Martinez³¹,
V. Lukashenko³¹, Y. Luo³, A. Lupato⁶¹, E. Luppi^{20,g}, O. Lupton⁵⁵, A. Lusiani^{28,t}, X. Lyu⁵,
L. Ma⁶, S. Maccolini^{19,e}, F. Machefert¹¹, F. Maciuc³⁶, V. Macko⁴⁸, P. Mackowiak¹⁴,
S. Maddrell-Mander⁵³, O. Madejczyk³⁴, L.R. Madhan Mohan⁵³, O. Maev³⁷, A. Maevskiy⁸¹,
D. Maisuzenko³⁷, M.W. Majewski³⁴, S. Malde⁶², B. Malecki⁴⁷, A. Malinin⁷⁹, T. Maltsev^{42,x},
H. Malygina¹⁶, G. Manca^{26,f}, G. Mancinelli¹⁰, R. Manera Escalero⁴⁴, D. Manuzzi^{19,e},
D. Marangotto^{25,q}, J. Maratas^{9,w}, J.F. Marchand⁸, U. Marconi¹⁹, S. Mariani^{21,47,h},
C. Marin Benito¹¹, M. Marinangeli⁴⁸, P. Marino⁴⁸, J. Marks¹⁶, P.J. Marshall⁵⁹, G. Martellotti³⁰,
L. Martinazzoli⁴⁷, M. Martinelli^{24,j}, D. Martinez Santos⁴⁵, F. Martinez Vidal⁴⁶, A. Massafferri¹,
M. Materok¹³, R. Matev⁴⁷, A. Mathad⁴⁹, Z. Mathe⁴⁷, V. Matiunin³⁸, C. Matteuzzi²⁴,
K.R. Mattioli⁸³, A. Mauri³¹, E. Maurice^{11,b}, J. Mauricio⁴⁴, M. Mazurek³⁵, M. McCann⁶⁰,
L. McConnell¹⁷, T.H. Mcgrath⁶¹, A. McNab⁶¹, R. McNulty¹⁷, J.V. Mead⁵⁹, B. Meadows⁶⁴,
C. Meaux¹⁰, G. Meier¹⁴, N. Meinert⁷⁵, D. Melnychuk³⁵, S. Meloni^{24,j}, M. Merk^{31,78}, A. Merli²⁵,
L. Meyer Garcia², M. Mikhasenko⁴⁷, D.A. Milanese⁷³, E. Millard⁵⁵, M.-N. Minard⁸,

L. Minzoni^{20,g}, S.E. Mitchell⁵⁷, B. Mitreska⁶¹, D.S. Mitzel⁴⁷, A. Mödden¹⁴, R.A. Mohammed⁶²,
 R.D. Moise⁶⁰, T. Mombächer¹⁴, I.A. Monroy⁷³, S. Monteil⁹, M. Morandin²⁷, G. Morello²²,
 M.J. Morello^{28,t}, J. Moron³⁴, A.B. Morris⁷⁴, A.G. Morris⁵⁵, R. Mountain⁶⁷, H. Mu³,
 F. Muheim⁵⁷, M. Mukherjee⁷, M. Mulder⁴⁷, D. Müller⁴⁷, K. Müller⁴⁹, C.H. Murphy⁶²,
 D. Murray⁶¹, P. Muzzetto²⁶, P. Naik⁵³, T. Nakada⁴⁸, R. Nandakumar⁵⁶, T. Nanut⁴⁸,
 I. Nasteva², M. Needham⁵⁷, I. Neri^{20,g}, N. Neri^{25,q}, S. Neubert⁷⁴, N. Neufeld⁴⁷, R. Newcombe⁶⁰,
 T.D. Nguyen⁴⁸, C. Nguyen-Mau^{48,n}, E.M. Niel¹¹, S. Nieswand¹³, N. Nikitin³⁹, N.S. Nolte⁴⁷,
 C. Nunez⁸³, A. Oblakowska-Mucha³⁴, V. Obraztsov⁴³, S. Ogilvy⁵⁸, D.P. O'Hanlon⁵³,
 R. Oldeman^{26,f}, C.J.G. Onderwater⁷⁷, J. D. Osborn⁸³, A. Ossowska³³, J.M. Otalora Goicochea²,
 T. Ovsiannikova³⁸, P. Owen⁴⁹, A. Oyanguren⁴⁶, B. Pagare⁵⁵, P.R. Pais⁴⁷, T. Pajero^{28,47,t},
 A. Palano¹⁸, M. Palutan²², Y. Pan⁶¹, G. Panshin⁸², A. Papanestis⁵⁶, M. Pappagallo⁵⁷,
 L.L. Pappalardo^{20,g}, C. Pappenheimer⁶⁴, W. Parker⁶⁵, C. Parkes⁶¹, C.J. Parkinson⁴⁵,
 B. Passalacqua²⁰, G. Passaleva^{21,47}, A. Pastore¹⁸, M. Patel⁶⁰, C. Patrignani^{19,e}, C.J. Pawley⁷⁸,
 A. Pearce⁴⁷, A. Pellegrino³¹, M. Pepe Altarelli⁴⁷, S. Perazzini¹⁹, D. Pereima³⁸, P. Perret⁹,
 K. Petridis⁵³, A. Petrolini^{23,i}, A. Petrov⁷⁹, S. Petrucci⁵⁷, M. Petruzzo²⁵, A. Philippov⁴¹,
 L. Pica²⁸, M. Piccini⁷⁶, B. Pietrzyk⁸, G. Pietrzyk⁴⁸, M. Pili⁶², D. Pinci³⁰, J. Pinzino⁴⁷,
 F. Pisani⁴⁷, A. Piucci¹⁶, Resmi P.K¹⁰, V. Placinta³⁶, S. Playfer⁵⁷, J. Plews⁵², M. Plo Casasus⁴⁵,
 F. Polci¹², M. Poli Lener²², M. Poliakov⁶⁷, A. Poluektov¹⁰, N. Polukhina^{80,c}, I. Polyakov⁶⁷,
 E. Polycarpo², G.J. Pomery⁵³, S. Ponce⁴⁷, A. Popov⁴³, D. Popov^{5,47}, S. Popov⁴¹,
 S. Poslavskii⁴³, K. Prasanth³³, L. Promberger⁴⁷, C. Prouve⁴⁵, V. Pugatch⁵¹, A. Puig Navarro⁴⁹,
 H. Pullen⁶², G. Punzi^{28,p}, W. Qian⁵, J. Qin⁵, R. Quagliani¹², B. Quintana⁸, N.V. Raab¹⁷,
 R.I. Rabadan Trejo¹⁰, B. Rachwal³⁴, J.H. Rademacker⁵³, M. Rama²⁸, M. Ramos Pernas⁴⁵,
 M.S. Rangel², F. Ratnikov^{41,81}, G. Raven³², M. Reboud⁸, F. Redi⁴⁸, F. Reiss¹²,
 C. Remon Alepuz⁴⁶, Z. Ren³, V. Renaudin⁶², R. Ribatti²⁸, S. Ricciardi⁵⁶, D.S. Richards⁵⁶,
 K. Rinnert⁵⁹, P. Robbe¹¹, A. Robert¹², G. Robertson⁵⁷, A.B. Rodrigues⁴⁸, E. Rodrigues⁵⁹,
 J.A. Rodriguez Lopez⁷³, M. Roehrken⁴⁷, A. Rollings⁶², P. Roloff⁴⁷, V. Romanovskiy⁴³,
 M. Romero Lamas⁴⁵, A. Romero Vidal⁴⁵, J.D. Roth⁸³, M. Rotondo²², M.S. Rudolph⁶⁷,
 T. Ruf⁴⁷, J. Ruiz Vidal⁴⁶, A. Ryzhikov⁸¹, J. Ryzka³⁴, J.J. Saborido Silva⁴⁵, N. Sagidova³⁷,
 N. Sahoo⁵⁵, B. Saitta^{26,f}, D. Sanchez Gonzalo⁴⁴, C. Sanchez Gras³¹, C. Sanchez Mayordomo⁴⁶,
 R. Santacesaria³⁰, C. Santamarina Rios⁴⁵, M. Santimaria²², E. Santovetti^{29,k}, D. Saranin⁸⁰,
 G. Sarpis⁶¹, M. Sarpis⁷⁴, A. Sarti³⁰, C. Satriano^{30,s}, A. Satta²⁹, M. Saur⁵, D. Savrina^{38,39},
 H. Sazak⁹, L.G. Scantlebury Smead⁶², S. Schael¹³, M. Schellenberg¹⁴, M. Schiller⁵⁸,
 H. Schindler⁴⁷, M. Schmelling¹⁵, T. Schmelzer¹⁴, B. Schmidt⁴⁷, O. Schneider⁴⁸, A. Schopper⁴⁷,
 M. Schubiger³¹, S. Schulte⁴⁸, M.H. Schune¹¹, R. Schwemmer⁴⁷, B. Sciascia²², A. Sciubba³⁰,
 S. Sellam⁶⁸, A. Semennikov³⁸, M. Senghi Soares³², A. Sergi^{52,47}, N. Serra⁴⁹, J. Serrano¹⁰,
 L. Sestini²⁷, A. Seuthe¹⁴, P. Seyfert⁴⁷, D.M. Shangase⁸³, M. Shapkin⁴³, I. Shchemerov⁸⁰,
 L. Shchutka⁴⁸, T. Shears⁵⁹, L. Shekhtman^{42,x}, Z. Shen⁴, V. Shevchenko⁷⁹, E.B. Shields^{24,j},
 E. Shmanin⁸⁰, J.D. Shupperd⁶⁷, B.G. Siddi²⁰, R. Silva Coutinho⁴⁹, L. Silva de Oliveira²,
 G. Simi²⁷, S. Simone^{18,d}, I. Skiba^{20,g}, N. Skidmore⁷⁴, T. Skwarnicki⁶⁷, M.W. Slater⁵²,
 J.C. Smallwood⁶², J.G. Smeaton⁵⁴, A. Smetkina³⁸, E. Smith¹³, M. Smith⁶⁰, A. Snoch³¹,
 M. Soares¹⁹, L. Soares Lavra⁹, M.D. Sokoloff⁶⁴, F.J.P. Soler⁵⁸, A. Solovev³⁷, I. Solovyev³⁷,
 F.L. Souza De Almeida², B. Souza De Paula², B. Spaan¹⁴, E. Spadaro Norella^{25,q}, P. Spradlin⁵⁸,
 F. Stagni⁴⁷, M. Stahl⁶⁴, S. Stahl⁴⁷, P. Stefko⁴⁸, O. Steinkamp^{49,80}, S. Stemmler¹⁶,
 O. Stenyakin⁴³, H. Stevens¹⁴, S. Stone⁶⁷, M.E. Stramaglia⁴⁸, M. Straticiu³⁶, D. Strelakina⁸⁰,
 S. Strokov⁸², F. Suljik⁶², J. Sun²⁶, L. Sun⁷², Y. Sun⁶⁵, P. Sviha⁶¹, P.N. Swallow⁵²,
 K. Swientek³⁴, A. Szabelski³⁵, T. Szumlak³⁴, M. Szymanski⁴⁷, S. Taneja⁶¹, Z. Tang³,
 T. Tekampe¹⁴, F. Teubert⁴⁷, E. Thomas⁴⁷, K.A. Thomson⁵⁹, M.J. Tilley⁶⁰, V. Tisserand⁹,
 S. T'Jampens⁸, M. Tobin⁶, S. Tolch⁴⁷, L. Tomassetti^{20,g}, D. Torres Machado¹, D.Y. Tou¹²,
 M. Traill⁵⁸, M.T. Tran⁴⁸, E. Trifonova⁸⁰, C. Trippl⁴⁸, A. Tsaregorodtsev¹⁰, G. Tuci^{28,p},
 A. Tully⁴⁸, N. Tuning³¹, A. Ukleja³⁵, D.J. Unverzagt¹⁶, A. Usachov³¹, A. Ustyuzhanin^{41,81},

U. Uwer¹⁶, A. Vagner⁸², V. Vagnoni¹⁹, A. Valassi⁴⁷, G. Valenti¹⁹, N. Valls Canudas⁴⁴,
M. van Beuzekom³¹, H. Van Hecke⁶⁶, E. van Herwijnen⁸⁰, C.B. Van Hulse¹⁷, M. van Veghel⁷⁷,
R. Vazquez Gomez⁴⁵, P. Vazquez Regueiro⁴⁵, C. Vázquez Sierra³¹, S. Vecchi²⁰, J.J. Velthuis⁵³,
M. Veltri^{21,r}, A. Venkateswaran⁶⁷, M. Veronesi³¹, M. Vesterinen⁵⁵, D. Vieira⁶⁴,
M. Vieites Diaz⁴⁸, H. Viemann⁷⁵, X. Vilasis-Cardona⁴⁴, E. Vilella Figueras⁵⁹, P. Vincent¹²,
G. Vitali²⁸, A. Vitkovskiy³¹, A. Vollhardt⁴⁹, D. Vom Bruch¹², A. Vorobyev³⁷, V. Vorobyev^{42,x},
N. Voropaev³⁷, R. Waldi⁷⁵, J. Walsh²⁸, C. Wang¹⁶, J. Wang³, J. Wang⁷², J. Wang⁴, J. Wang⁶,
M. Wang³, R. Wang⁵³, Y. Wang⁷, Z. Wang⁴⁹, D.R. Ward⁵⁴, H.M. Wark⁵⁹, N.K. Watson⁵²,
S.G. Weber¹², D. Websdale⁶⁰, C. Weisser⁶³, B.D.C. Westhenry⁵³, D.J. White⁶¹,
M. Whitehead⁵³, D. Wiedner¹⁴, G. Wilkinson⁶², M. Wilkinson⁶⁷, I. Williams⁵⁴,
M. Williams^{63,69}, M.R.J. Williams⁶¹, F.F. Wilson⁵⁶, W. Wislicki³⁵, M. Witek³³, L. Witola¹⁶,
G. Wormser¹¹, S.A. Wotton⁵⁴, H. Wu⁶⁷, K. Wyllie⁴⁷, Z. Xiang⁵, D. Xiao⁷, Y. Xie⁷, H. Xing⁷¹,
A. Xu⁴, J. Xu⁵, L. Xu³, M. Xu⁷, Q. Xu⁵, Z. Xu⁵, Z. Xu⁴, D. Yang³, Y. Yang⁵, Z. Yang³,
Z. Yang⁶⁵, Y. Yao⁶⁷, L.E. Yeomans⁵⁹, H. Yin⁷, J. Yu⁷, X. Yuan⁶⁷, O. Yushchenko⁴³,
K.A. Zarebski⁵², M. Zavertyaev^{15,c}, M. Zdybal³³, O. Zenaiev⁴⁷, M. Zeng³, D. Zhang⁷,
L. Zhang³, S. Zhang⁴, Y. Zhang⁴⁷, Y. Zhang⁶², A. Zhelezov¹⁶, Y. Zheng⁵, X. Zhou⁵, Y. Zhou⁵,
X. Zhu³, V. Zhukov^{13,39}, J.B. Zonneveld⁵⁷, S. Zucchelli^{19,e}, D. Zuliani²⁷, G. Zunica⁶¹.

¹Centro Brasileiro de Pesquisas Físicas (CBPF), Rio de Janeiro, Brazil

²Universidade Federal do Rio de Janeiro (UFRJ), Rio de Janeiro, Brazil

³Center for High Energy Physics, Tsinghua University, Beijing, China

⁴School of Physics State Key Laboratory of Nuclear Physics and Technology, Peking University, Beijing, China

⁵University of Chinese Academy of Sciences, Beijing, China

⁶Institute Of High Energy Physics (IHEP), Beijing, China

⁷Institute of Particle Physics, Central China Normal University, Wuhan, Hubei, China

⁸Univ. Grenoble Alpes, Univ. Savoie Mont Blanc, CNRS, IN2P3-LAPP, Annecy, France

⁹Université Clermont Auvergne, CNRS/IN2P3, LPC, Clermont-Ferrand, France

¹⁰Aix Marseille Univ, CNRS/IN2P3, CPPM, Marseille, France

¹¹Université Paris-Saclay, CNRS/IN2P3, IJCLab, Orsay, France

¹²LPNHE, Sorbonne Université, Paris Diderot Sorbonne Paris Cité, CNRS/IN2P3, Paris, France

¹³I. Physikalisches Institut, RWTH Aachen University, Aachen, Germany

¹⁴Fakultät Physik, Technische Universität Dortmund, Dortmund, Germany

¹⁵Max-Planck-Institut für Kernphysik (MPIK), Heidelberg, Germany

¹⁶Physikalisches Institut, Ruprecht-Karls-Universität Heidelberg, Heidelberg, Germany

¹⁷School of Physics, University College Dublin, Dublin, Ireland

¹⁸INFN Sezione di Bari, Bari, Italy

¹⁹INFN Sezione di Bologna, Bologna, Italy

²⁰INFN Sezione di Ferrara, Ferrara, Italy

²¹INFN Sezione di Firenze, Firenze, Italy

²²INFN Laboratori Nazionali di Frascati, Frascati, Italy

²³INFN Sezione di Genova, Genova, Italy

²⁴INFN Sezione di Milano-Bicocca, Milano, Italy

²⁵INFN Sezione di Milano, Milano, Italy

²⁶INFN Sezione di Cagliari, Monserrato, Italy

²⁷Università degli Studi di Padova, Università e INFN, Padova, Padova, Italy

²⁸INFN Sezione di Pisa, Pisa, Italy

²⁹INFN Sezione di Roma Tor Vergata, Roma, Italy

³⁰INFN Sezione di Roma La Sapienza, Roma, Italy

³¹Nikhef National Institute for Subatomic Physics, Amsterdam, Netherlands

³²Nikhef National Institute for Subatomic Physics and VU University Amsterdam, Amsterdam, Netherlands

³³Henryk Niewodniczanski Institute of Nuclear Physics Polish Academy of Sciences, Kraków, Poland

³⁴AGH - University of Science and Technology, Faculty of Physics and Applied Computer Science, Kraków, Poland

- ³⁵ *National Center for Nuclear Research (NCBJ), Warsaw, Poland*
- ³⁶ *Horia Hulubei National Institute of Physics and Nuclear Engineering, Bucharest-Magurele, Romania*
- ³⁷ *Petersburg Nuclear Physics Institute NRC Kurchatov Institute (PNPI NRC KI), Gatchina, Russia*
- ³⁸ *Institute of Theoretical and Experimental Physics NRC Kurchatov Institute (ITEP NRC KI), Moscow, Russia, Moscow, Russia*
- ³⁹ *Institute of Nuclear Physics, Moscow State University (SINP MSU), Moscow, Russia*
- ⁴⁰ *Institute for Nuclear Research of the Russian Academy of Sciences (INR RAS), Moscow, Russia*
- ⁴¹ *Yandex School of Data Analysis, Moscow, Russia*
- ⁴² *Budker Institute of Nuclear Physics (SB RAS), Novosibirsk, Russia*
- ⁴³ *Institute for High Energy Physics NRC Kurchatov Institute (IHEP NRC KI), Protvino, Russia, Protvino, Russia*
- ⁴⁴ *ICCUB, Universitat de Barcelona, Barcelona, Spain*
- ⁴⁵ *Instituto Galego de Física de Altas Enerxías (IGFAE), Universidade de Santiago de Compostela, Santiago de Compostela, Spain*
- ⁴⁶ *Instituto de Física Corpuscular, Centro Mixto Universidad de Valencia - CSIC, Valencia, Spain*
- ⁴⁷ *European Organization for Nuclear Research (CERN), Geneva, Switzerland*
- ⁴⁸ *Institute of Physics, Ecole Polytechnique Fédérale de Lausanne (EPFL), Lausanne, Switzerland*
- ⁴⁹ *Physik-Institut, Universität Zürich, Zürich, Switzerland*
- ⁵⁰ *NSC Kharkiv Institute of Physics and Technology (NSC KIPT), Kharkiv, Ukraine*
- ⁵¹ *Institute for Nuclear Research of the National Academy of Sciences (KINR), Kyiv, Ukraine*
- ⁵² *University of Birmingham, Birmingham, United Kingdom*
- ⁵³ *H.H. Wills Physics Laboratory, University of Bristol, Bristol, United Kingdom*
- ⁵⁴ *Cavendish Laboratory, University of Cambridge, Cambridge, United Kingdom*
- ⁵⁵ *Department of Physics, University of Warwick, Coventry, United Kingdom*
- ⁵⁶ *STFC Rutherford Appleton Laboratory, Didcot, United Kingdom*
- ⁵⁷ *School of Physics and Astronomy, University of Edinburgh, Edinburgh, United Kingdom*
- ⁵⁸ *School of Physics and Astronomy, University of Glasgow, Glasgow, United Kingdom*
- ⁵⁹ *Oliver Lodge Laboratory, University of Liverpool, Liverpool, United Kingdom*
- ⁶⁰ *Imperial College London, London, United Kingdom*
- ⁶¹ *Department of Physics and Astronomy, University of Manchester, Manchester, United Kingdom*
- ⁶² *Department of Physics, University of Oxford, Oxford, United Kingdom*
- ⁶³ *Massachusetts Institute of Technology, Cambridge, MA, United States*
- ⁶⁴ *University of Cincinnati, Cincinnati, OH, United States*
- ⁶⁵ *University of Maryland, College Park, MD, United States*
- ⁶⁶ *Los Alamos National Laboratory (LANL), Los Alamos, United States*
- ⁶⁷ *Syracuse University, Syracuse, NY, United States*
- ⁶⁸ *Laboratory of Mathematical and Subatomic Physics, Constantine, Algeria, associated to ²*
- ⁶⁹ *School of Physics and Astronomy, Monash University, Melbourne, Australia, associated to ⁵⁵*
- ⁷⁰ *Pontifícia Universidade Católica do Rio de Janeiro (PUC-Rio), Rio de Janeiro, Brazil, associated to ²*
- ⁷¹ *Guangdong Provincial Key Laboratory of Nuclear Science, Institute of Quantum Matter, South China Normal University, Guangzhou, China, associated to ³*
- ⁷² *School of Physics and Technology, Wuhan University, Wuhan, China, associated to ³*
- ⁷³ *Departamento de Física, Universidad Nacional de Colombia, Bogota, Colombia, associated to ¹²*
- ⁷⁴ *Universität Bonn - Helmholtz-Institut für Strahlen und Kernphysik, Bonn, Germany, associated to ¹⁶*
- ⁷⁵ *Institut für Physik, Universität Rostock, Rostock, Germany, associated to ¹⁶*
- ⁷⁶ *INFN Sezione di Perugia, Perugia, Italy, associated to ²⁰*
- ⁷⁷ *Van Swinderen Institute, University of Groningen, Groningen, Netherlands, associated to ³¹*
- ⁷⁸ *Universiteit Maastricht, Maastricht, Netherlands, associated to ³¹*
- ⁷⁹ *National Research Centre Kurchatov Institute, Moscow, Russia, associated to ³⁸*
- ⁸⁰ *National University of Science and Technology "MISIS", Moscow, Russia, associated to ³⁸*
- ⁸¹ *National Research University Higher School of Economics, Moscow, Russia, associated to ⁴¹*
- ⁸² *National Research Tomsk Polytechnic University, Tomsk, Russia, associated to ³⁸*
- ⁸³ *University of Michigan, Ann Arbor, United States, associated to ⁶⁷*

^a *Universidade Federal do Triângulo Mineiro (UFMT), Uberaba-MG, Brazil*

^b *Laboratoire Leprince-Ringuet, Palaiseau, France*

^c *P.N. Lebedev Physical Institute, Russian Academy of Science (LPI RAS), Moscow, Russia*

- ^d *Università di Bari, Bari, Italy*
- ^e *Università di Bologna, Bologna, Italy*
- ^f *Università di Cagliari, Cagliari, Italy*
- ^g *Università di Ferrara, Ferrara, Italy*
- ^h *Università di Firenze, Firenze, Italy*
- ⁱ *Università di Genova, Genova, Italy*
- ^j *Università di Milano Bicocca, Milano, Italy*
- ^k *Università di Roma Tor Vergata, Roma, Italy*
- ^l *AGH - University of Science and Technology, Faculty of Computer Science, Electronics and Telecommunications, Kraków, Poland*
- ^m *DS4DS, La Salle, Universitat Ramon Llull, Barcelona, Spain*
- ⁿ *Hanoi University of Science, Hanoi, Vietnam*
- ^o *Università di Padova, Padova, Italy*
- ^p *Università di Pisa, Pisa, Italy*
- ^q *Università degli Studi di Milano, Milano, Italy*
- ^r *Università di Urbino, Urbino, Italy*
- ^s *Università della Basilicata, Potenza, Italy*
- ^t *Scuola Normale Superiore, Pisa, Italy*
- ^u *Università di Modena e Reggio Emilia, Modena, Italy*
- ^v *Università di Siena, Siena, Italy*
- ^w *MSU - Iligan Institute of Technology (MSU-IIT), Iligan, Philippines*
- ^x *Novosibirsk State University, Novosibirsk, Russia*
- ^y *INFN Sezione di Trieste, Trieste, Italy*
- ^z *Universidad Nacional Autónoma de Honduras, Tegucigalpa, Honduras*